

## Article

# A New Transmitting Coil for Powering Endoscopic Capsules Using Wireless Power Transfer

Tommaso Campi <sup>1,\*</sup>, Silvano Cruciani <sup>2</sup>, Francesca Maradei <sup>3</sup> and Mauro Feliziani <sup>1</sup>

<sup>1</sup> Department of Industrial and Information Engineering and Economics, University of L'Aquila, Poggio Roio, 67100 L'Aquila, Italy

<sup>2</sup> Department of Industrial Engineering, Tor Vergata University of Rome, Via del Politecnico 1, 00133 Rome, Italy

<sup>3</sup> Department of Astronautics, Electrical and Energetics Engineering, Sapienza University of Rome, Via Eudossiana 18, 00185 Rome, Italy

\* Correspondence: tommaso.campi@univaq.it; Tel.: +39-0862-434421

**Abstract:** This study focuses on using wireless power transfer (WPT) technology based on magnetic resonant coupling (MRC) to supply electric power to an endoscopic capsule to be used for the direct feeding of specific functions or for battery charging. One of the main limitations of the diffusion of endoscopic capsules is the limited autonomy of the internal battery. The aim of the paper is to present an innovative system to wirelessly power capsules using inductive coupling. Here, a new transmitting coil architecture is proposed to allow the wireless charging of the capsule equipped with a monoaxial receiving coil for any possible geometric position and orientation. The new wearable transmitting coil consists of four rectangular coils with independent excitations, and it is capable of producing a magnetic field in any direction. The obtained results in terms of electrical performance of the proposed WPT system and in terms of in situ electromagnetic physical quantities are compared with the basic restrictions of electromagnetic field (EMF) safety guidelines. The results obtained are very promising, as the proposed WPT configuration can transfer at least 250 mW in a capsule that travels along the entire gastrointestinal tract.

**Keywords:** endoscopic capsule; coil design; deep implant; electromagnetic field (EMF) safety; inductive coupling; magnetic resonant coupling (MRC); numerical dosimetry; wireless power transfer (WPT)



**Citation:** Campi, T.; Cruciani, S.; Maradei, F.; Feliziani, M. A New Transmitting Coil for Powering Endoscopic Capsules Using Wireless Power Transfer. *Electronics* **2023**, *12*, 1942. <https://doi.org/10.3390/electronics12081942>

Academic Editor: Fabio Corti

Received: 28 March 2023

Revised: 13 April 2023

Accepted: 17 April 2023

Published: 20 April 2023



**Copyright:** © 2023 by the authors. Licensee MDPI, Basel, Switzerland. This article is an open access article distributed under the terms and conditions of the Creative Commons Attribution (CC BY) license (<https://creativecommons.org/licenses/by/4.0/>).

## 1. Introduction

Wireless power transfer (WPT) systems are used for the transmission of electrical energy without the use of any galvanic connection. There are several technologies that can be used for WPT, mainly classified into near-field and far-field WPT systems. The latter are used for the transmission of energy over long distances and are mainly based on radio frequency (RF), microwave (MW) or laser technologies, while in the near-field WPT, power is transferred by magnetic fields using inductive coupling (IC), which is also called magnetic coupling (MC), or by electric fields using capacitive coupling (CC). These two couplings can also operate under resonant conditions to improve the electrical performance; in this case, they are called magnetic resonant coupling (MRC) [1–4] and capacitive resonant coupling (CRC).

Nowadays, the most diffused technology for short-range power transmissions is the MRC, since it permits very good electrical performance and has a limited number of safety problems. There are several applications of this technology [5,6], including the wireless power supply of biomedical devices such as endoscopic capsules. Endoscopic capsules are small, swallowable devices that can contain a camera, sensors and actuators, and are used for diagnosis and therapy of the gastrointestinal tract [7–11]. Electronic capsules require a power source to operate, which is generally an integrated battery. However, the internal battery is often not large enough to allow all possible electronic or electrically

driven operations. Therefore, some capsule functions are often disabled to save energy. A potential solution to this issue is the use of the WPT-MRC technology.

An important feature of using WPT-MRC technology for endoscopic capsules is the safety and reliability of power transmission [12–35]. Unlike other WPT methods, such as laser-based power transmission, WPT-MRC does not use ionizing radiation, which can be harmful to the body. In addition, WPT-MRC is not affected by environmental factors, such as humidity or temperature, which can affect the performance of other wireless power transfer methods.

In a typical WPT-MRC system, two coils are used, a transmitting coil and a receiving coil, to transfer power according to Faraday's law of induction. By using compensation capacitors, the coils are designed to resonate at the same frequency, enabling efficient energy transfer. When the transmitting coil is powered with an alternating current (AC), a magnetic field is created. This time-varying magnetic field induces an AC voltage in the receiver coil, which is rectified to power the endoscopic capsule. In the typical architecture, the transmitting coil is placed on the patient's skin, while the receiving coil is placed in the capsule. The distance between the coils is variable and depends on the instantaneous position of the endoscopic capsule during its travel through the entire length of the intestines and on the anatomical conformation of the patient's body. These distances can be very different, from about 2 cm to more than 10 cm. Such a significant distance is a real challenge for the WPT due to attenuation of the magnetic field that occurs in biological tissues. With WPT technology, the capsule can be continuously powered, as long as it is within range of the transmitting coil.

Despite these advantages, there are also some limitations to using a WPT system to power endoscopic capsules, the most critical of which are the range and the amount of power that can be transferred to a deep implant without exceeding the electromagnetic field (EMF) safety limits, known as basic restrictions in International Commission on Non-Ionizing Radiation Protection (ICNIRP) guidelines [36,37]. If the power transfer is limited, it may not be sufficient to recharge the battery and to power all the sensors and devices in the capsule. To overcome these limitations, an adequate design of the WPT system is required.

The most challenging design choices are:

- Selection of the operational frequency;
- Configuration of the receiving coil;
- Configuration of the transmitting coil.

A key aspect in designing a WPT-MRC system is the frequency at which it operates and resonates. The frequency must be carefully chosen, taking into account different and often opposite phenomena. Typically, for WPT-MRC systems, the frequency used is in the range from a few kilohertz to a few megahertz. In the present work, the frequency of 500 kHz is adopted as is a good compromise between coupling and losses [4]. Once the resonant frequency has been determined, the transmitting and receiving coils can be designed to effectively operate at this frequency.

The physical size and shape are very important to the design of the receiving coil. The coil must be small enough to be integrated into the capsule to be powered, while also receiving enough power for the device's operations. In the considered case, the receiving coil must be small enough to be mounted on the external surface of the cylindrical capsule, which typically has a diameter of about 1 cm and a length of 2–2.5 cm. This can be challenging, as coil size is proportional to power. Therefore, a trade-off must be made between coil size and power level. Another important consideration is whether the receiving coil should be uniaxial or triaxial. The monoaxial coil can effectively pick up an incident magnetic field only if it is parallel to the axis of the cylindrical capsule, while the triaxial coil can pick up an incident magnetic field having any arbitrary direction.

To save space and weight in the capsule, the monoaxial solution is adopted in this work, and therefore the challenge is in the design of the transmitting coil to produce a magnetic field that has all non-zero rectangular components anywhere in the intestine so that the monoaxial receiving coil can pick it up for any position and orientation of

the capsule. Clearly, the shape of the transmitting coil affects the WPT performance. A planar coil generates a nearly monoaxial magnetic field, and is therefore not suitable for this kind of application. However, this limitation can be overcome by optimizing the design of the coils and using more than one transmitting coil. In this work, we use four rectangular coils that can be independently excited to produce a magnetic field inside the human body with all non-zero rectangular components, as explained in the following sections. There are mainly two advantages of the proposed excitation system: a monoaxial receiving coil permits researchers to miniaturize the components that need to be installed on the capsule, as a receiving coil based on triaxial coil should require a lot of space and a more complex electronic unit to handle all the three windings [17–29]. The second important advantage is the possibility to easily adapt the system to different human body conformations, while maintaining very good uniformity of the field inside the body for all the three field components. In the work presented in [30], a transmitting coil was presented, which produced magnetic fields with all three components; however, it was very difficult to wear by the patient and could not be easily adapted to different body sizes.

The paper is organized as follows. First, the proposed setup for a wireless power system for an endoscopic capsule and the WPT methodology are presented. The configuration of the secondary coil placed on the capsule is then illustrated, and an in-depth description of the architecture of the transmitting coil and of the system electronics is proposed. In the results section, a test case is considered using numerical simulations to predict the electrical performance of the system. Finally, an investigation into the safety aspects is presented.

## 2. Materials and Methods

### 2.1. System Configuration

While higher frequencies allow the reduction in the size of electronic circuitry and increased electromagnetic coupling, there are some critical drawbacks such as:

- Increased power loss in electronic components, conductors and nearby metallic objects due to eddy currents;
- An increase in the specific absorption rate (SAR) in the human body;
- An increase in the magnetic field emission in the environment;
- A reduction of the penetration depth inside the body (not ideal for deep implants).

Here, the operating frequency and design of the receiving coil are selected on the basis of previous studies [4]. An operating frequency of a few hundred kilohertz has been proven in [4] to be the best compromise between the limitation of power losses in the electronics, the relatively low power level to be transferred to the internal device and the large distance between the coils when the capsule is deep in the human body. Thus, in this investigation a resonant frequency  $f_0 = 500$  kHz is adopted for the WPT-MRC system.

There are several works in the technical literature on the wireless powering of an endoscopic capsule, but most of them adopt a circular or a rectangular planar coil for the transmitter [13–22]. This coil configuration mainly produces a monoaxial field so it is necessary to equip the receiver with a triaxial coil to always pick up the incident magnetic field in an arbitrary direction. This solution is not very convenient as the increased size and weight of the receiving coil may not always be acceptable for a capsule. In our work, we adopt a different solution. For the architecture of the system, the basic idea is to use a monoaxial helicoidal receiving coil wound on the outer casing of the capsule, capable of picking up an incident magnetic field whose direction is parallel to that of the axis of the cylindrical capsule. The receiver with pick-up coil and the battery are integrated in the capsule, while the transmitter coil is placed outside the human body and powered by a primary source of electricity. Since the receiving coil is monoaxial, the transmitting coil must generate a magnetic field with all non-zero orthogonal components anywhere in the gastrointestinal tract to be sure the battery charging process is effective. To this aim, an original transmitting system is here proposed based on an array of four independent transmitting coils, as shown in Figure 1. The WPT system is designed to deliver power

greater than  $P_{out} = 250$  mW to the load with a voltage level of  $V_{out} = 2$  V for any orientation and position of the capsule.

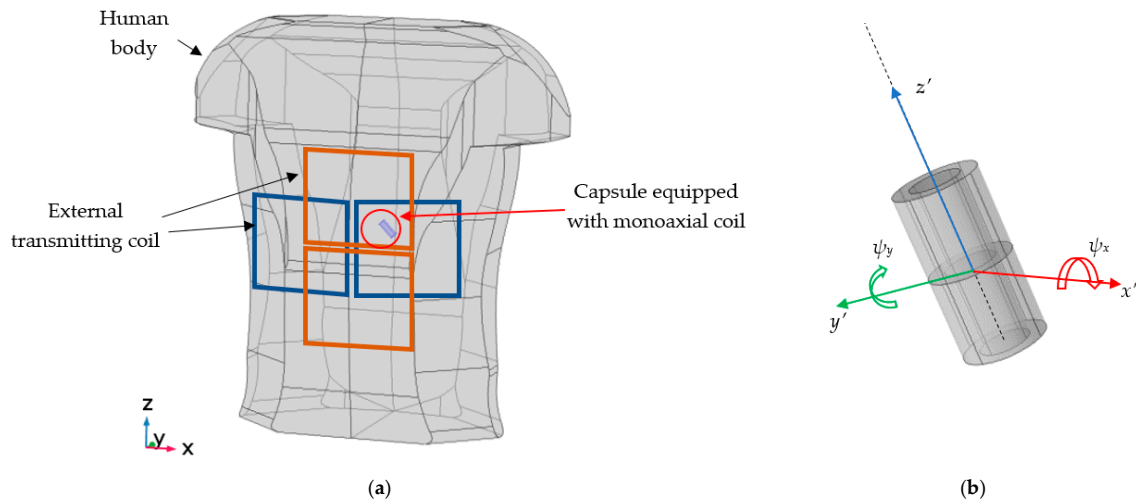


**Figure 1.** Proposed WPT setup. (a) Transmitter coil array consisting of 4 wearable rectangular coils. (b) Local coordinate system for a cylindrical capsule.

### 2.2. WPT Receiver Design

The aim of the proposed work is the design of a transmitting coil able to allow the use of a simple, compact and light receiver. In the past, biaxial or triaxial receiver coils were used to collect the wirelessly transmitted power for any inclination of the capsule. Here, to reduce the size and weight, the receiver coil consists of a monoaxial coil wound around the capsule. Since the magnetic field produced by the receiving coil current is too small to change the incident field generated by the transmitting coil current, the magnetic coupling can be approximated by a unidirectional link, from transmitter to receiver, usually known as weak coupling.

In this study, a capsule with an external diameter of  $d_c = 10$  mm and length  $l_c = 25$  mm is considered. The capsule is composed of a central cylinder with two hemispheres on the top and bottom faces of the cylinder, so as to have a capsule with no edges that could produce lacerations to the biological tissue, and at the same time, with a hydrodynamic shape. The two hemispheres are made of silicone to allow the incorporation of sensors such as a camera, etc. The cylinder part of the capsule is covered by a ferrite layer (i.e., hollow cylinder) of height  $h_e = 20$  mm and thickness  $t_{fe} = 1$  mm. A sketch of the capsule configuration is shown in Figure 2.

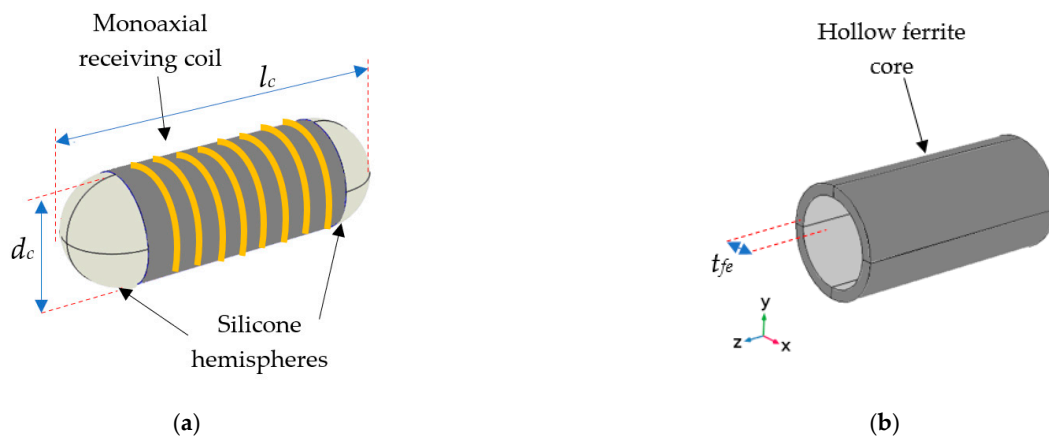


**Figure 2.** Capsule with monoaxial coil (in yellow) wound over a layer of ferrite covering the body of the cylindrical capsule (a) and layer of ferrite (b).

It should be noted that in the configuration presented in [38], the capsule was completely made of ferrite to improve the performance of the WPT; however, it implied that the ferrite occupied the entire available space, so it could be used as a “power module” in the case of multiple robotic capsule modules when functions are divided and shared in a modular robotic system [8]. For a single module capsule configuration, the hollow ferrite cylinder adopted here is preferable.

The design of the receiving coil must take into account the electrical specifications of the load that it needs to supply and the geometric constraints. The maximum power required from the capsule mainly depends on the instruments and functions installed (camera, robotic functions for locomotion, additional functions for diagnostics and therapy, radio link, etc.), and it can reach 1 W, although 500 mW may often be sufficient. However, the maximum power required to recharge the battery integrated in the capsule can reasonably be set at 250 mW.

The receiving coil energized by the external field can be modeled as a voltage source  $E_2$ , which models the electromotive force produced by the incident time-varying magnetic flux produced by the transmitting coil, connected in series with the self-inductance,  $L_2$ , and the equivalent series resistance,  $R_2$ , of the receiving coil. The value of the electromotive force can be calculated as  $E_2 = -j\omega N_2\phi$ , with  $\omega = 2\pi f$ ,  $f$  being the frequency, and  $\phi$  being the incident flux linked with the  $N_2$  turns of the receiving coil. Weak coupling is valid when the capsule draws a relatively small amount of power, so that the induced current is small and unable to change the magnetic field distribution.

To improve the performance in terms of power transferred, the inductive reactance of the coil is fully compensated by an additional capacitor connected in series,  $C_2$ , which is calculated as:

$$C_2 = \frac{1}{\omega_0^2 L_2} \quad (1)$$

where  $\omega_0 = 2\pi f_0$ , and  $f_0$  is the resonance frequency.

The voltage level required by the load can be obtained by suitably choosing the number of turns  $N_2$ , with  $E_2$  being proportional to  $N_2$ . Alternatively, an electronic converter can be used, but it takes up space and reduces reliability. In the proposed system, a full-wave voltage doubler (rectifier) is adopted. This topology has two main advantages: a DC voltage that is twice the size of the AC voltage and the use of only two passive components (diodes). The DC values of the voltage  $V_{out}$  and current  $I_{out}$  at the output of the rectifier can be calculated with the AC electrical quantities as:

$$V_{out} = 2\left(\sqrt{2}V_2 - 2V_{drop}\right) \quad (2)$$

$$I_{out} = \frac{\sqrt{2}I_2}{2} \quad (3)$$

where  $V_2$  and  $I_2$  are the rms values of the voltage and current at the output port of the compensated receiving coil, respectively, and  $V_{drop}$  is the forward voltage drop on the diode. The complete equivalent circuit is shown in Figure 3.

At resonance, the voltage across inductor and capacitor can be neglected, obtaining the following mesh voltage equation:

$$V_2 = E_2 - R_2 I_2 \quad (4)$$

which can be handled as

$$V_2 = N_2 E_2' - N_2 R_2' I_2 \quad (5)$$

where  $E_2'$  and  $R_2'$  are the induced voltage and the resistance per turn of the receiving coil, respectively. Thus, it yields:

$$N_2 = \frac{V_2}{E_2' - R_2' I_2} \quad (6)$$

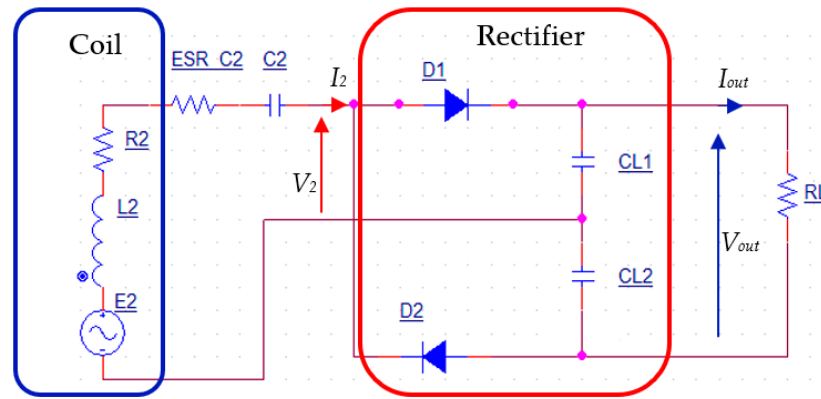


Figure 3. Complete electric schematic of the receiver.

The number of turns  $N_2$  can be rewritten, considering the presence of the rectifier, in terms of DC quantities via (2) and (3) as:

$$N_2 = \frac{\frac{V_{out}}{2} + 2V_{drop}}{\sqrt{2E_2' - 2R_2' I_{out}}} \tag{7}$$

The DC equivalent resistance can be calculated by  $R_L = V_{out}^2 / P_{out}$ , with  $V_{out}$  being the DC voltage level and  $P_{out}$  being the power of the load. The DC current can be calculated by  $I_{out} = P_{out} / V_{out}$ . From (7), it is possible to select the optimal number of turns  $N_2$  for the receiving coil. In the design phase, the receiving coil is sized considering the point in the intestine where the magnetic flux linked to the  $N_2$  turns is minimal, thus ensuring that the required power can be transferred to the capsule at whatever point during its travel through the gastrointestinal tract. When the linked flux increases, the output voltage also increases; thus, the electronic unit on the transmitter reduces the transmitting power to avoid system overload.

### 2.3. WPT Transmitter

#### 2.3.1. Simulation Set-Up

The magnetic and electric fields are simulated using a commercial 3D FEM solver. Supposing that the domain is composed only by linear isotropic homogeneous materials, the magnetic and electric fields inside and outside the human body can be studied with the following equations using the AC/DC module of COMSOL Multiphysics:

$$\nabla \times \mathbf{B} = \mu \mathbf{J} \tag{8}$$

$$\nabla \cdot \mathbf{J} = 0 \tag{9}$$

$$\mathbf{J} = (\sigma + j\omega\epsilon)\mathbf{E} + \mathbf{J}_e \tag{10}$$

$$\mathbf{E} = -\nabla V - j\omega \mathbf{A} \tag{11}$$

$$\mathbf{B} = \nabla \times \mathbf{A} \tag{12}$$

where  $\mathbf{J}$  is the current density,  $\mathbf{E}$  is the electric field,  $\mathbf{A}$  is the magnetic vector potential,  $\mathbf{J}_e$  is the external current density source,  $\mathbf{B}$  is the magnetic flux density,  $\sigma$  is the electrical conductivity,  $\mu$  is the magnetic permeability and  $\epsilon$  is the electric permittivity.

A tetrahedral mesh has been adopted, and the number of elements used is equal to 245,210. In order to perform the parametric analysis, a Parametric Sweep has been

performed using the position of the capsule (orientation, distance, etc.) and different excitation modes for the primary coil as parameters.

### 2.3.2. Coil Design

The design of the transmitting system is of paramount importance for the realization of a reliable power supply of the endoscopic capsules. Three main aspects should be considered:

1. The primary magnetic field should cover a large area within the body, including the entire gastrointestinal tract;
2. The inclination of the capsule varies while it travels through the intestine; thus, it is necessary to produce a primary magnetic field with non-zero components along three orthogonal directions;
3. Compliance with the electromagnetic field (EMF) safety standards.

As mentioned before, here, we adopt a simple monoaxial pick-up coil mounted on the capsule and focus the attention on developing an efficient transmitter suitable to provide a magnetic field with non-zero components in the three orthogonal directions. An interesting solution achieving this goal was presented in [38], where a birdcage architecture was used to generate all non-zero field components inside the body, but it required a complex geometrical and electronic configuration. In this work, a much simpler solution is provided. The main idea is to adopt a multicoil transmitter based on two adjacent coils, similar to the double D (DD) coil configuration. To evaluate the field produced by a pair of coils, it is possible to use the superposition between the fields produced by the two coils. There is an analytical solution to calculate the magnetic field produced by a rectangular coil of dimensions  $a \times b$  in free space. This can be used for a first estimate of magnetic field levels and is easily implemented in numerical software such as MATLAB or OCTAVE. The magnetic flux density at point  $P(x, y, z)$ , considering the Cartesian coordinate system with orientations as shown in Figure 4 (i.e., the rectangular coil lies on the  $xz$  plane at  $y = y_0$ ), is given by [39]:

$$B_x(x, y, z) = \alpha \sum_{i=1}^4 (-1)^{i+1} \frac{y - y_0}{r_i(r_i + z_i)} \quad (13)$$

$$B_y(x, y, z) = \alpha \sum_{i=1}^4 (-1)^i \frac{r_i(z_i + x_i) + z_i^2 + x_i^2}{r_i(r_i + z_i)(r_i + x_i)} \quad (14)$$

$$B_z(x, y, z) = \alpha \sum_{i=1}^4 (-1)^{i+1} \frac{y - y_0}{r_i(r_i + x_i)} \quad (15)$$

where  $\alpha = \mu_0 NI / (4\pi)$ ,  $I$  is the current flowing in the coil,  $N$  is the number of turns and where  $z_1 = z_4 = z + a/2$ ,  $z_2 = z_3 = z - a/2$ ,  $x_1 = x_2 = x + b/2$ , and  $x_3 = x_4 = x - b/2$ , and where  $r_i$  is the distance between the  $i$ -th corner of the coil and the observation point  $r_i(x, y, z) = \sqrt{x_i^2 + z_i^2 + (y - y_0)^2}$ . We can assume, for simplicity, that the plane of the coil is at the position  $y = y_0 = 0$  and that the center of the coil coincides with the origin of the axis. With some simple translation and using the superposition theorem, we can calculate the magnetic field produced by the primary coil at any point of the lossless domain. It should be noted that (9)–(11) can be used successfully even in biological tissues when the penetration depth is large, i.e., at a relatively low frequency.

The DD coil consists of two adjacent planar rectangular coils with mesh currents in the opposite direction and generates the main magnetic field parallel to the coil plane, as shown in Figure 5a. In this work, this kind of energization is called series excitation. However, the two adjacent rectangular coils, indicated as #1A and #1B, can also be energized in such a way as to have identical mesh current directions (antiseriess excitation), producing a magnetic field which has the principal component on the vertical axis, as shown in Figure 5b.

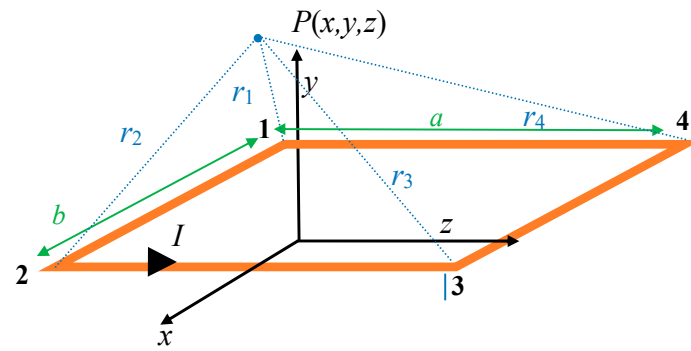


Figure 4. Magnetic flux density produced by a rectangular coil.

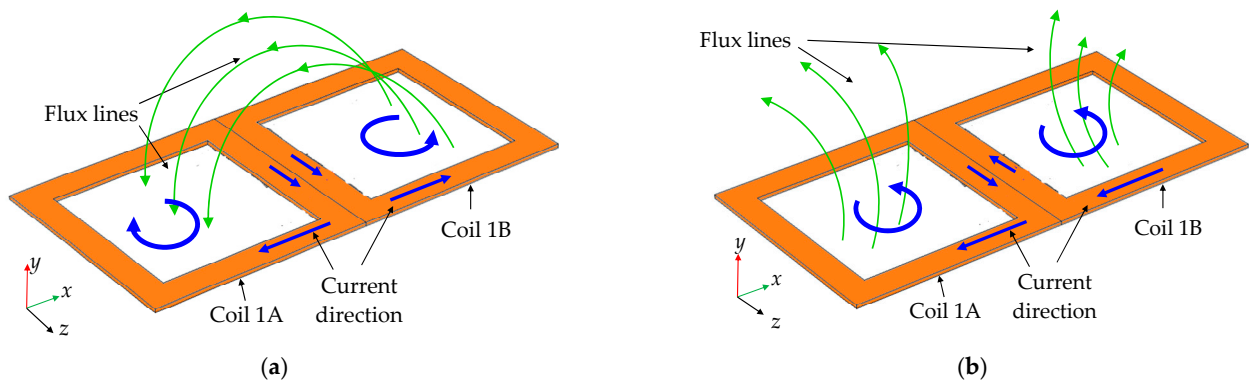


Figure 5. Magnetic flux line (in green) of DD coil with opposite mesh current directions (a) and identical mesh current directions (b).

To create non-zero magnetic field components in all orthogonal axes, another identical structure of two adjacent square coils is placed in geometric quadrature with the first double coil structure, resulting in an array structure with four independent coils, as shown in Figure 6a. The structure sketch of the body-mounted (wearable) coil array adapted to the shape of the human body is shown in Figure 6b, where the simplified model of an adult torso is considered. This last model is composed of a cylinder with an elliptical base, made up of muscle with the electromagnetic physical constants taken from the IT'IS database for the considered frequency [40].

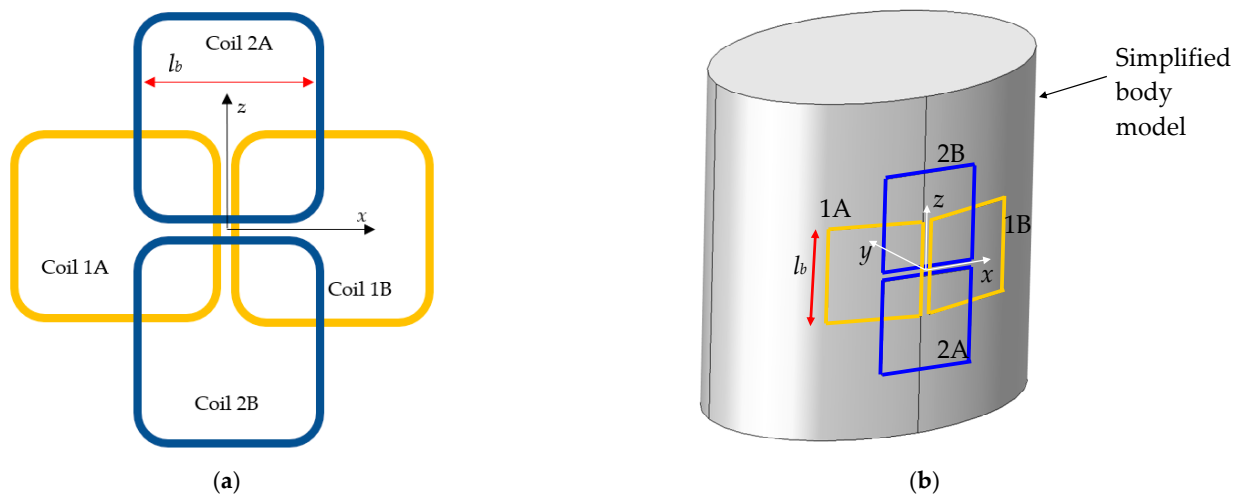
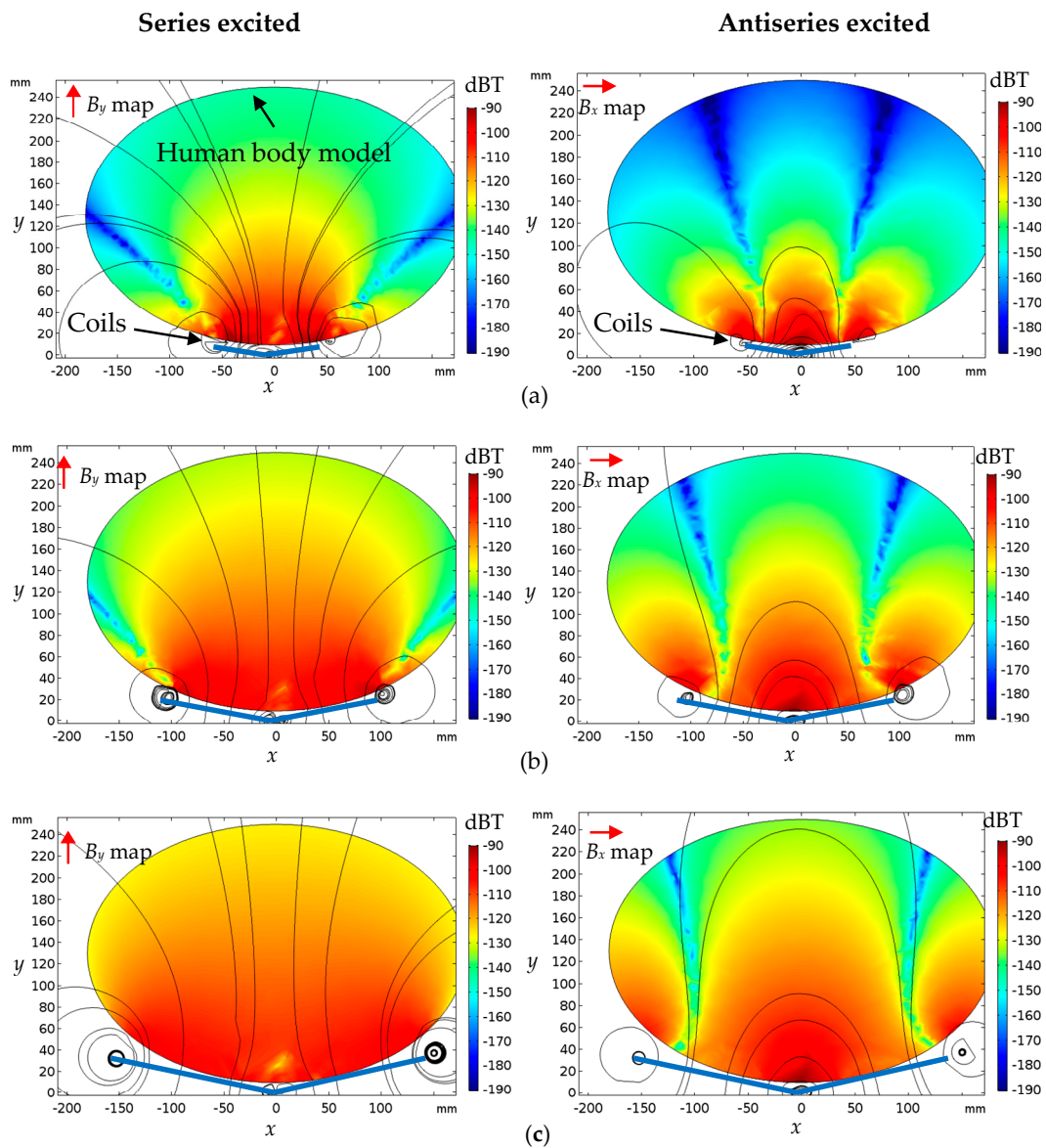


Figure 6. Proposed four coil array configuration (a) and application of the coil array on the human torso (b).



To get an overview of the behavior of the magnetic field produced by the 4-coil array structure, only the coils #1A and #1B are first energized to perform a sensitive analysis on the influence of the coil size on the magnetic field distribution. The center of the four coil array structure is assumed to be the origin (0, 0, 0) of the coordinate axes. All square coils are assumed identical with side lengths  $l_b$ . Three different coil side lengths are considered:  $l_b = 50$  mm, 100 mm and 150 mm. For simplicity, a single turn coil is adopted with unitary current. The maps of the magnetic flux density components  $B_x$  (series excitation) and  $B_y$  (antiseries excitation) on the  $xy$  plane at  $z = 0$  are shown in Figure 7. As can be seen the use of larger coil ( $l_b = 150$  mm) permits to obtain a very wide magnetic field coverage where the capsule can be easily energized. Please note that to allow a better adaptation of the coils to the human torso, the two coils #1A and #1B are not perfectly planar as in Figure 5, but form an angle of less than  $180^\circ$ .



**Figure 7.** Strength lines and amplitude maps of  $B_y$  (series excited, on the left) and  $B_x$  (antiseries excited, on the right) for different coil side length:  $l_b = 50$  mm (a),  $l_b = 100$  mm (b) and  $l_b = 150$  mm (c).

After this preliminary investigation, the coils #2A and #2B are similarly energized to generate the  $z$  component of the magnetic field. The  $B_z$  map when coils #2A and #2B are excited in series is shown in Figure 8. It should be noted how each pair of coils (#1A-#1B

or #2A-#2B) can be powered alone or in combination with the other pair of coils to obtain different preferential directions of the magnetic field.

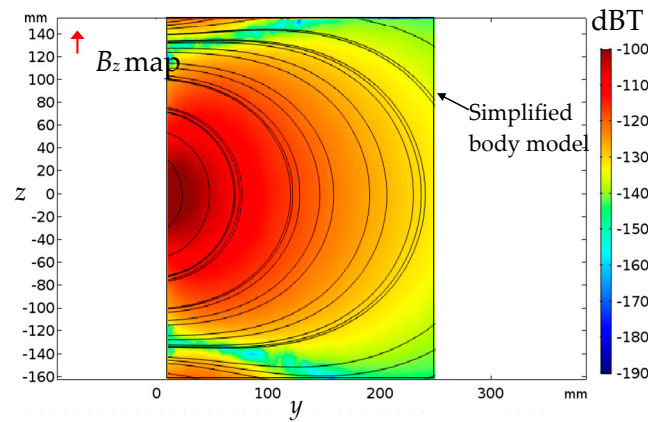


**Figure 8.** Magnetic flux density strength lines and amplitude maps of  $B_z$  (series excited) for coil side length:  $l_b = 150$  mm.

### 2.3.3. Electronic Configuration

The proposed coil configuration requires specific electronic unit to work properly. As previously described, each pair of adjacent coils can operate independently, and the two coils of the same pair can in turn be energized in series or antiseriess. To energize the transmitter coil array, a power supply system based on a full bridge inverter and six switches is proposed, as schematically shown in Figure 9.

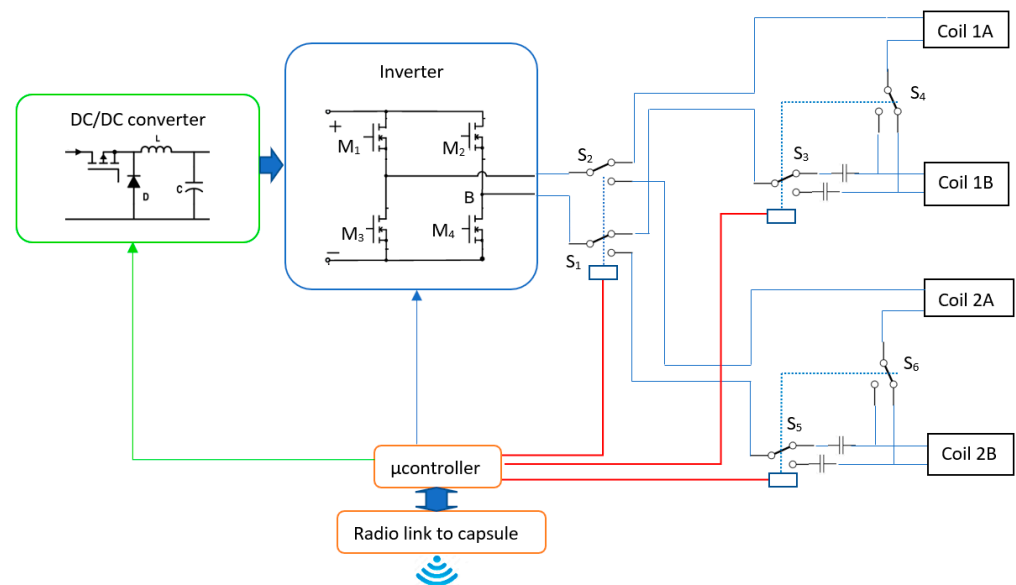


**Figure 9.** Proposed electronic configuration of the transmitter side.

Switches  $S_1$  and  $S_2$  can be simultaneously activated to energize coils #1A-#1B or #2A-#2B, while switches  $S_3$ - $S_4$  and switches  $S_5$ - $S_6$  can be simultaneously activated to select the series or anti-series excitation in each pair. Since the coils connected in series or antiseriess can have different configurations, different capacitors are adopted to reach the resonance conditions. A microcontroller is used to select switches for proper energizing of the coil array. Before the inverter is used, a DC/DC converter is adopted to adjust the voltage level, and then the transmitted power.

The capsule, which is already equipped with a microcontroller and a data link for the telemetry, is used also for the control of the power transmission procedure. The proposed algorithm works as described in the following:

Initially the transmitter polls all possible coil excitations (e.g., coils #1A and #1B in series or antiseriess, coil #2A and #2B in series or antiseriess) adopting low power condition. The level of the power is adjusted by varying the duty cycle of the DC/DC converter. During the polling process, the receiver registers the configuration with the highest transmission power. To read a correct value, the polling phase is assumed to have a duration of  $100T$ , where  $T = 1/f$  is the period of the signal. The total polling time for the four configurations is  $t_p = 0.8$  ms. At the end of the procedure, the receiver sends back to the transmitter the configuration code that produces a better performance. The transmitter selects the best coil configuration by selecting switches and starts the power transmission. In this phase, the capsule continuously sends the received power level, which is used by the transmitter to adjust the power level. This process continues until a new poll is taken (e.g., after 1 s). This algorithm is based on the assumption that the movement of the capsule within the human body is typically much slower than the polling intervals.

### 3. Results

A demonstrative configuration is presented using the excitation system described in Section 2.3. The transmission system consists of four coils, each of them having  $N = 10$  turns, and made using litz wire to reduce the AC losses and heating. The coil side length is set at  $l_b = 150$  mm. The parameters of each couple of transmitting coils (#1A-#1B and #2A-#2B) are: self-inductances,  $L_{AB} = 54.2$   $\mu\text{H}$ , and self-resistance,  $R_{AB} = 240$  m $\Omega$ . Note how the mutual coupling between coils #1A-#1B and coils #2A-#2B is not considered since when one pair of coils is transmitting, the other is open (current equal to zero); therefore, it interferes a very small amount with the transmitting pair of coils. The capsule is sized and shaped as described in Section 2.2 and is positioned within the torso model. The main objective of the work is to energize the capsule inside a cube with side  $l = 20$  cm within the body model, containing the entire gastrointestinal tract, as shown in Figure 10a. The problem configuration of the simplified human body model, including the capsule and the coil array structure, is modeled in COMSOL numerical software [41]. The first test is aimed at calculating the magnetic field inside the box. To perform this analysis, the minimum value of the orthogonal components of the magnetic flux density (i.e.,  $B_x$ ,  $B_y$ , and  $B_z$ ) is calculated in the box for each possible excitation, as shown in Table 1. It should be noted that the results obtained for each B component for different excitations are very different, demonstrating the effectiveness of the proposed transmitting coil configuration. At the end of the calculation process, the excitation that allows the maximum value for each field component (highlighted in red) is assumed as the worst case (almost proportional to the minimum connected flux) for the design of the receiving coil to guarantee 250 mW to the load.

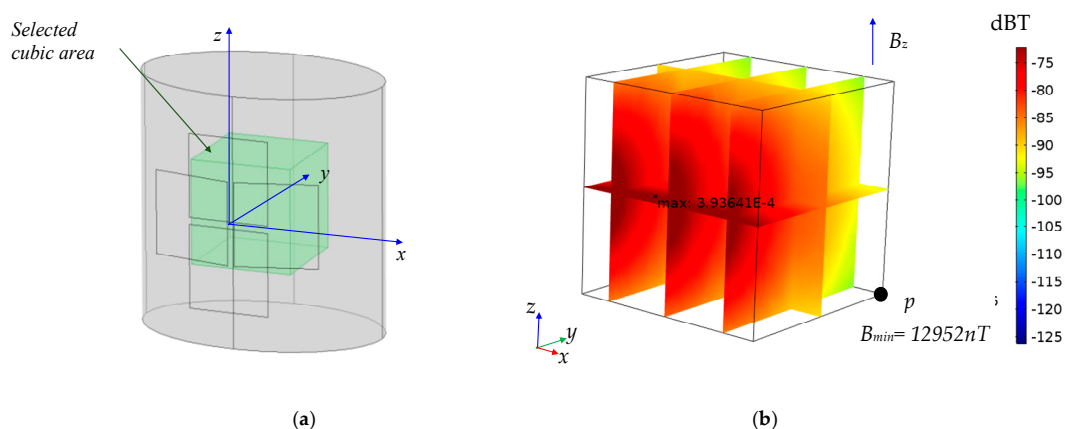


**Figure 10.** Selected cubic region inside the torso (a); distribution of  $B_z$  inside the cubic region for the worst case scenario (b).

**Table 1.** Minimum value of the B field components in the cubic region inside the human body for different excitation of the coil array structure. The maximum B field for each component is highlighted in red.

Excitation	B <sub>x</sub> (nT)	B <sub>y</sub> (nT)	B <sub>z</sub> (nT)
#1A-#1B coils, series	1.4446	<b>36418</b>	2.1492
#1A-#1B coils, antiseriess	<b>14151</b>	9.9482	1.1311
#2A-#2B coils, series	2.2954	27107	0.43686
#2A-#2B coils, antiseriess	0.56196	1.6051	<b>12952</b>

The minimum value is obtained for the z component of magnetic flux induction,  $B_{z,min} = 12.952 \mu\text{T}$ , at point  $p$  shown in Figure 10b. The excitation algorithm is based on the idea of maximizing magnetic coupling between the transmitting coil and the receiving coil for any position and inclination of the capsule by selecting the most appropriate excitation among the four available. However, to design the receiving coil, it is of fundamental importance to know the minimum magnetic flux linkage produced by each excitation for any inclination of the capsule. The magnetic flux is calculated by positioning the capsule at point  $p$  of minimum field considering various inclinations of the capsule with respect to its center (see again Figure 1b) in both directions orthogonal to the z axis ( $\psi_x = 0^\circ, 30^\circ, 45^\circ, 60^\circ$  and  $90^\circ$ ;  $\psi_y = 0^\circ, 30^\circ, 45^\circ, 60^\circ$  and  $90^\circ$ ) and for the four different excitations.

For each inclination, the excitation that maximizes the magnetic flux (and therefore the power transferred) is selected. This polling procedure is automated by the microcontroller. The worst case scenario is obtained when the capsule is in position  $p$  with an inclination of  $\psi_x = 30^\circ$  and  $\psi_y = 45^\circ$  when coils #1A-#1B are activated and connected in series. In this condition, the linked flux is equal to 18.2 nWb. This value, assumed as the minimum linked flux, is used to calculate the number of turns  $N_2$  of the receiving coil according to (7). The system has been designed to deliver a nominal power to the load,  $P_{out} = 250 \text{ mW}$ , a load voltage of  $V_{out} = 2 \text{ V}$  and a current  $I_{out} = P_{out}/V_{out} = 0.125 \text{ A}$ . First, a wire capable of tolerating a current carrying capacity of  $I_2 = 0.176 \text{ A}$  in (3) is selected for the receiving coils. To reduce the losses and heating, a litz wire composed of 10 strands of AWG 48 wire (equivalent wire diameter  $d = 0.2 \text{ mm}$ ) was considered with a per-unit-length (p.u.l.) wire resistance of  $R_{2pul} = 1048 \text{ m}\Omega/\text{m}$ . This litz wire configuration is suitable for a maximum current equal to  $I_2$  at the frequency of 500 kHz. Then, the number of turns,  $N_2 = 60$ , is calculated by using (7). The load is modeled as a resistor  $R_L = V_{out}^2/P_{out} = 16 \Omega$ . The calculated parameters of the receiving coil are:  $L_2 = 148 \mu\text{H}$  and  $R_2 = 1.63 \Omega$ . The compensation capacitor that ensures resonance is  $C_2 = 684 \text{ pF}$  [4].

The circuit parameter values are used in the equivalent electrical circuit model (see again Figure 3) to evaluate the electrical performance of the system. The output voltage  $V_{out}$ , the voltage before the rectifier  $V_2$  and the load power  $P_{out}$  are shown in Figure 11. The obtained output power is  $P_{out} = 238 \text{ mW}$ , which is slightly lower than the design value. However, it was evaluated on the basis of the worst case magnetic coupling between the transmitting and receiving coils inside the selected volume. Therefore, it is reasonable to assume that the average power value is much higher than 238 mW and certainly higher than 250 mW, which is the design value. Additionally, the electrical efficiency of the system can be calculated as the ratio between the power delivered to the capsule and the input port of the transmitting coils. Considering the same worst case position, the minimum efficiency is 8.3%. It should be noted that the results obtained with the combined FEM and circuital analysis were validated by measurements taken by the same authors of several works [4,38]. Finally, the electrical performance has been calculated considering the mean value of the magnetic flux in the selected area considering the capsule aligned with the z-axis. The mean value of the magnetic flux is 35.3 nWb. The circuit analysis has been repeated, adopting this value of magnetic flux obtaining an output power equal to  $P_{mean} = 1.42 \text{ W}$ , with a mean efficiency  $\eta_{mean} = 0.48\%$ . Obviously, this power is too high and cannot be easily managed by the secondary coil and by the electronic circuit; thus, the transmitted power should be

reduced adjusting the parameters of the DC/DC converter (e.g., by reducing the input voltage before the inverter), such as described in the explanation of the algorithm.

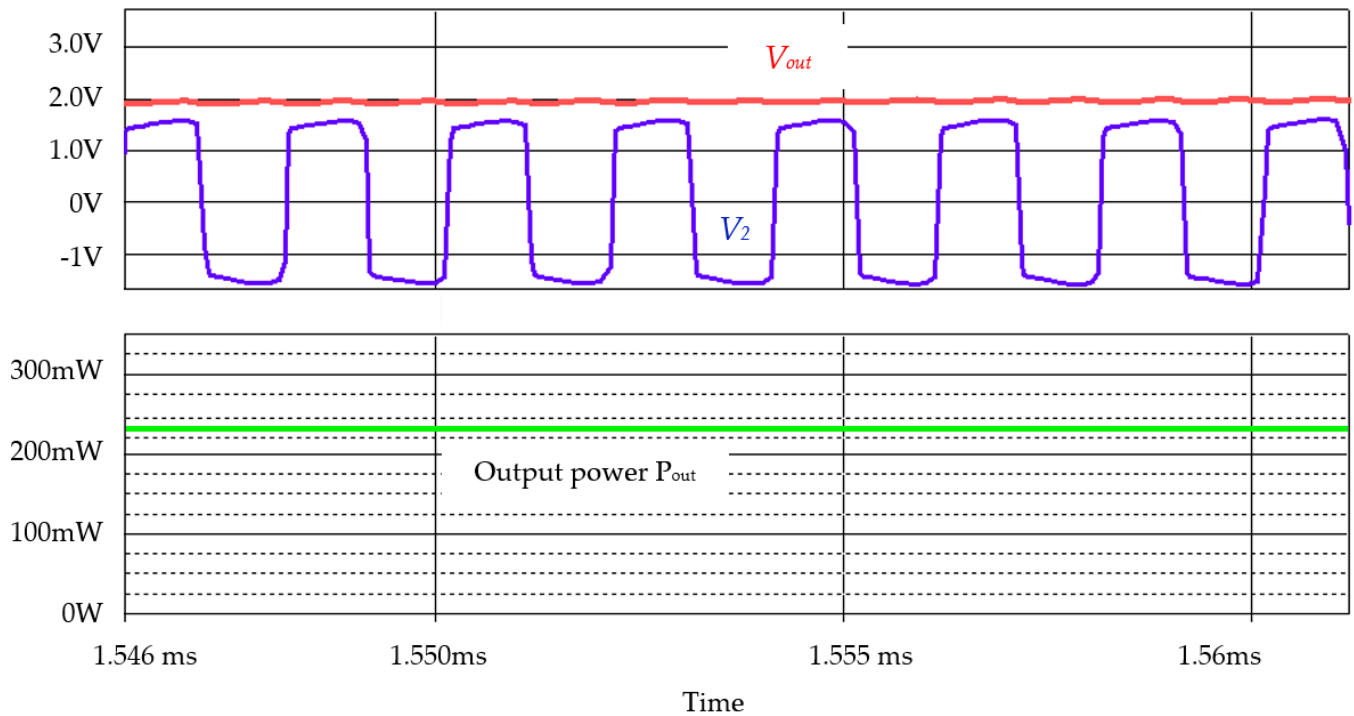


**Figure 11.** Waveform of the output voltage before the rectifier (blu), on the load (red) and the output power (green).

As a final step of the proposed investigation, a preliminary study on electromagnetic field (EMF) safety is provided to check the compliance of the proposed four-coil array transmitter. The ICNIRP guidelines assess the compliance in terms of internal electric field  $E$  and specific absorption ratio (SAR) at the considered frequency of 500 kHz. Both internal electric field  $E$  and SAR are numerically calculated solving the Equation (8) by the finite element method (FEM), assuming the coil currents as magnetic field sources [42–47].

The maximum internal electric field  $E$  and SAR are calculated as:

$$E_{\max} = \max(\|\mathbf{E}(x, y, z)\|) \quad (16)$$

$$SAR_{\max} = \max\left(\frac{\sigma(x, y, z)}{\rho(x, y, z)} \|\mathbf{E}(x, y, z)\|^2\right) \quad (17)$$

where  $\mathbf{E}(x, y, z)$  is the electric field vector in biological tissues,  $\sigma$  is the conductivity and  $\rho$  is the mass density of the considered tissue (i.e., muscle for the sake of simplicity in this preliminary investigation). According to the ICNIRP guidelines [36,37],  $E$  and SAR must be taken as the 99th percentile or averaged in 10 g of continuous tissue, respectively. The basic restrictions are  $E = 40.5$  V/m and  $SAR = 2$  W/kg at the resonant frequency of  $f_0 = 500$  kHz. In the current analysis, a more restrictive precautionary condition is applied as the evaluation is performed without adopting percentile or averaging the field, i.e., in terms of maximum values. The maximum electric field inside the trunk obtained from the calculations is  $E = 27.5$  V/m and the maximum SAR is 0.94 W/kg, which are both well below the basic restrictions. The distribution of  $E$  and SAR inside the torso are shown in Figure 12.

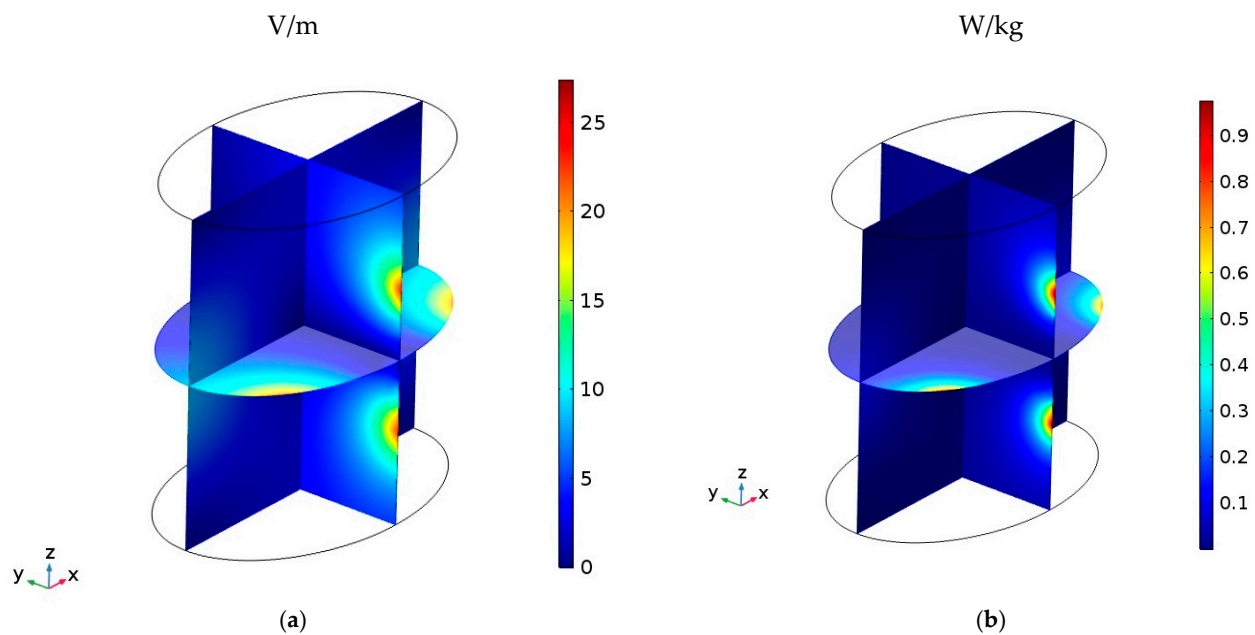


**Figure 12.** Distribution of electric field  $E$  (a) and SAR (b) inside the torso.

#### 4. Conclusions

A new transmitting coil architecture has been proposed for wireless power transfer of endoscopic capsules to recharge their battery, while avoiding the current limitations of electrically driven functions for diagnostics and therapy due to limited available electrical energy.

The new transmitting coil array consists of four rectangular planar coils with independent excitations. It is able to produce a magnetic field in any direction, thus ensuring that the required power is wirelessly transferred to the capsule, equipped by a monoaxial coil, at any point and for any orientation in the gastrointestinal tract.

The proposed WPT system operates at 500 kHz and can power the capsule with approximately 250 mW at 2 V over a large area within the body. Preliminary numerical investigations have demonstrated the satisfactory electrical performance of the proposed system and compliance with EMF safety limits.

The advantages of the proposed method are mainly represented by the modularity of the feeding system, which easily adapts to the different anatomical configurations of the patient and allows specialists to customize the area to be fed inside the body. The future development of the system involves implementing and testing the system on a demonstrator. With further research and development, wireless power transfer could revolutionize the field of endoscopy and offer new opportunities for capsule robots to diagnose and treat therapies, even with microsurgical techniques.

**Author Contributions:** T.C., S.C., F.M. and M.F. conceived, planned the experiments and carried out the simulations. All authors provided critical feedback, improved the final design, analyzed the data and wrote the paper. All authors have read and agreed to the published version of the manuscript.

**Funding:** This research received no external funding.

**Data Availability Statement:** This research was funded by the Projects of national interest—PRIN2017, Project title “WPT4WID: Wireless Power Transfer for Wearable and Implantable Devices”, under Project no. 2017YJE9XK.

**Conflicts of Interest:** The authors declare no conflict of interest.

## References

1. Stankiewicz, J.M.; Choroszucho, A. Comparison of the Efficiency and Load Power in Periodic Wireless Power Transfer Systems with Circular and Square Planar Coils. *Energies* **2021**, *14*, 4975. [[CrossRef](#)]
2. Sun, L.; Ma, D.; Tang, H. A review of recent trends in wireless power transfer technology and its applications in electric vehicle wireless charging. *Renew. Sustain. Energy Rev.* **2018**, *91*, 490–503. [[CrossRef](#)]
3. Wang, C.-S.; Covic, G.; Stielau, O. Power Transfer Capability and Bifurcation Phenomena of Loosely Coupled Inductive Power Transfer Systems. *IEEE Trans. Ind. Electron.* **2004**, *51*, 148–157. [[CrossRef](#)]
4. Campi, T.; Cruciani, S.; De Santis, V.; Maradei, F.; Feliziani, M. Near Field Wireless Powering of Deep Medical Implants. *Energies* **2019**, *12*, 2720. [[CrossRef](#)]
5. Campi, T.; Cruciani, S.; De Santis, V.; Maradei, F.; Feliziani, M. Numerical characterization of the magnetic field in electric vehicles equipped with a WPT system. *Wirel. Power Transf.* **2017**, *4*, 78–87. [[CrossRef](#)]
6. Campi, T.; Cruciani, S.; Maradei, F.; Feliziani, M. Wireless Charging System Integrated in a Small Unmanned Aerial Vehicle (UAV) with High Tolerance to Planar Coil Misalignment. In Proceedings of the 2019 Joint International Symposium on Electromagnetic Compatibility, Sapporo and Asia-Pacific International Symposium on Electromagnetic Compatibility (EMC Sapporo/APEMC), Sapporo, Japan, 3–7 June 2019; pp. 601–604. [[CrossRef](#)]
7. Menciassi, A.; Iacovacci, V. Implantable biorobotic organs. *APL Bioeng.* **2020**, *4*, 040402. [[CrossRef](#)] [[PubMed](#)]
8. Moglia, A.; Menciassi, A.; Dario, P.; Cuschieri, A. Capsule endoscopy: Progress update and challenges ahead. *Nat. Rev. Gastroenterol. Hepatol.* **2009**, *6*, 353–361. [[CrossRef](#)]
9. Mapara, S.S.; Patravale, V.B. Medical capsule robots: A renaissance for diagnostics, drug delivery and surgical treatment. *J. Control. Release* **2017**, *261*, 337–351. [[CrossRef](#)]
10. Carta, R.; Tortora, G.; Thoné, J.; Lenaerts, B.; Valdastris, P.; Menciassi, A.; Dario, P.; Puers, R. Wireless powering for a self-propelled and steerable endoscopic capsule for stomach inspection. *Biosens. Bioelectron.* **2009**, *25*, 845–851. [[CrossRef](#)]
11. Swain, P. The future of wireless capsule endoscopy. *World J. Gastroenterol.* **2008**, *14*, 4142–4145. [[CrossRef](#)]
12. Li, H.; Yan, G.; Ma, G. An active endoscopic robot based on wireless power transmission and electromagnetic localization. *Int. J. Med. Robot. Comput. Assist. Surg.* **2008**, *4*, 355–367. [[CrossRef](#)] [[PubMed](#)]
13. Ryu, M.; Kim, J.D.; Chin, H.U.; Kim, J.; Song, S.Y. Three-dimensional power receiver for in vivo robotic capsules. *Med. Biol. Eng. Comput.* **2007**, *45*, 997–1002. [[CrossRef](#)] [[PubMed](#)]
14. Carta, R.; Thoné, J.; Puers, R. A wireless power supply system for robotic capsular endoscopes. *Sens. Actuators A Phys.* **2010**, *162*, 177–183. [[CrossRef](#)]
15. Pan, G.; Xin, W.; Yan, G.; Chen, J. A video wireless capsule endoscopy system powered wirelessly: Design, analysis and experiment. *Meas. Sci. Technol.* **2011**, *22*, 065802. [[CrossRef](#)]
16. Xin, W.; Yan, G.; Wang, W. Study of a wireless power transmission system for an active capsule endoscope. *Int. J. Med. Robot. Comput. Assist. Surg.* **2010**, *6*, 113–122. [[CrossRef](#)]
17. Puers, R.; Carta, R.; Thoné, J. Wireless power and data transmission strategies for next-generation capsule endoscopes. *J. Micromech. Microeng.* **2011**, *21*, 054008. [[CrossRef](#)]
18. Miah, S.; Jayathurathnage, P.; Icheln, C.; Haneda, K.; Tretyakov, S. High-Efficiency Wireless Power Transfer System for Capsule Endoscope. In Proceedings of the 2019 13th International Symposium on Medical Information and Communication Technology (ISMICT), Oslo, Norway, 8–10 May 2019; pp. 1–5. [[CrossRef](#)]
19. Basar, R.; Ahmad, M.Y.; Cho, J.; Ibrahim, F. Application of Wireless Power Transmission Systems in Wireless Capsule Endoscopy: An Overview. *Sensors* **2014**, *14*, 10929–10951. [[CrossRef](#)]
20. Carta, R.; Sfakiotakis, M.; Pateromichelakis, N.; Thoné, J.; Tsakiris, D.; Puers, R. A multi-coil inductive powering system for an endoscopic capsule with vibratory actuation. *Sensors Actuators A Phys.* **2011**, *172*, 253–258. [[CrossRef](#)]
21. Jourand, P.; Puers, R. A Class-E driven inductive power delivery system covering the complete upper body. *Sens. Actuators A Phys.* **2012**, *183*, 132–139. [[CrossRef](#)]
22. Puga, R.; Dinis, M.; Ferreira, J.; Pontes, L.; Lomba, E. Wireless power transfer endoscopy capsule—CAP4U. *Heal. Technol.* **2018**, *9*, 45–55. [[CrossRef](#)]
23. Fang, X.; Liu, H.; Li, G.; Shao, Q.; Li, H. Wireless power transfer system for capsule endoscopy based on strongly coupled magnetic resonance theory. In Proceedings of the 2011 IEEE International Conference on Mechatronics and Automation, Beijing, China, 7–10 August 2011; pp. 232–236. [[CrossRef](#)]
24. Na, K.; Jang, H.; Ma, H.; Bien, F. Tracking Optimal Efficiency of Magnetic Resonance Wireless Power Transfer System for Biomedical Capsule Endoscopy. *IEEE Trans. Microw. Theory Tech.* **2014**, *63*, 295–304. [[CrossRef](#)]
25. Sun, T.; Xie, X.; Li, G.; Gu, Y.; Deng, Y.; Wang, Z. A Two-Hop Wireless Power Transfer System With an Efficiency-Enhanced Power Receiver for Motion-Free Capsule Endoscopy Inspection. *IEEE Trans. Biomed. Eng.* **2012**, *59*, 3247–3254. [[CrossRef](#)]
26. Murliky, L.; Oliveira, G.; de Sousa, F.R.; Brusamarello, V.J. Tracking and Dynamic Tuning of a Wireless Powered Endoscopic Capsule. *Sensors* **2022**, *22*, 6924. [[CrossRef](#)]
27. Chen, F.; Jiang, P.; Yan, G.; Wang, W.; Meng, Y. Design of Multi-Coil Wireless Power Transfer System for Gastrointestinal Capsule Robot. *J. Shanghai Jiaotong Univ. (Sci.)* **2021**, *26*, 76–83. [[CrossRef](#)]
28. Basar, R.; Ahmad, M.Y.; Cho, J.; Ibrahim, F. An improved resonant wireless power transfer system with optimum coil configuration for capsule endoscopy. *Sens. Actuators A Phys.* **2016**, *249*, 207–216. [[CrossRef](#)]

29. Basar, M.R.; Ahmad, M.Y.; Cho, J.; Ibrahim, F. An Improved Wearable Resonant Wireless Power Transfer System for Bio-medical Capsule Endoscope. *IEEE Trans. Ind. Electron.* **2018**, *65*, 7772–7781. [[CrossRef](#)]
30. Wen, F.; Chu, X.; Li, Q.; Jing, F.; Zhao, W.; Chu, Z. Receiver Localization and Power Stabilization for Wireless Power Transfer System. In Proceedings of the 2020 IEEE International Conference on Applied Superconductivity and Electromagnetic Devices (ASEMD), Tianjin, China, 16–18 October 2020; pp. 1–2.
31. Sravya, D.; Bobba, P.B.; Rani, M.N.S. Investigation of Wireless Power Transfer System with Different Coil Structures used in Wireless Capsule Endoscope. In Proceedings of the 2021 International Conference on Sustainable Energy and Future Electric Transportation (SEFET), Hyderabad, India, 21–23 January 2021; pp. 1–6.
32. Cui, C.; Zhao, Q.; Li, Z. Design of Wireless Power Supply Optimized Structure for Capsule Endoscopes. *J. Power Technol.* **2016**, *96*, 101–109.
33. Campi, T.; Cruciani, S.; Santilli, G.P.; Feliziani, M. Numerical analysis of EMF safety and thermal aspects in a pacemaker with a Wireless Power Transfer system. In Proceedings of the 2015 IEEE Wireless Power Transfer Conference (WPTC), Boulder, CO, USA, 13–15 May 2015; pp. 1–4. [[CrossRef](#)]
34. Campi, T.; Cruciani, S.; Palandrani, F.; De Santis, V.; Hirata, A.; Feliziani, M. Wireless Power Transfer Charging System for AIMDs and Pacemakers. *IEEE Trans. Microw. Theory Tech.* **2016**, *64*, 633–642. [[CrossRef](#)]
35. Campi, T.; Cruciani, S.; De Santis, V.; Feliziani, M. EMF Safety and Thermal Aspects in a Pacemaker Equipped With a Wireless Power Transfer System Working at Low Frequency. *IEEE Trans. Microw. Theory Tech.* **2016**, *64*, 375–382. [[CrossRef](#)]
36. International Commission on Non-Ionizing Radiation Protection. Guidelines for limiting exposure to time-varying electric and magnetic fields for low frequencies (1 Hz–100 kHz). *Health Phys.* **2010**, *99*, 818–836. [[CrossRef](#)]
37. International Commission on Non-Ionizing Radiation Protection (ICNIRP). Guidelines for Limiting Exposure to Electromagnetic Fields (100 kHz to 300 GHz). *Health Phys.* **2020**, *118*, 483–524. [[CrossRef](#)] [[PubMed](#)]
38. Campi, T.; Cruciani, S.; Maradei, F.; Feliziani, M. Innovative Wireless Charging System for Implantable Capsule Robots. *IEEE Trans. Electromagn. Compat.* **2021**, *63*, 1726–1734. [[CrossRef](#)]
39. Cruciani, S.; Maradei, F.; Feliziani, M. Assessment of magnetic field levels generated by a wireless power transfer (WPT) system at 20 kHz. In Proceedings of the 2013 IEEE International Symposium on Electromagnetic Compatibility, Denver, CO, USA, 5–9 August 2013; pp. 259–264. [[CrossRef](#)]
40. Hasgall, P.A.; Neufeld, E.; Gosselin, M.C.; Klingenböck, A.; Kuster, N. IT’IS Database for Thermal and Electromagnetic Parameters of Biological Tissues, Version 2.6. *IT’IS, Zurich, Switzerland*. 13 January 2020. Available online: [www.itis.ethz.ch/database](http://www.itis.ethz.ch/database) (accessed on 21 February 2023).
41. COMSOL Multiphysics. Available online: <https://www.comsol.it> (accessed on 14 January 2023).
42. Gosselin, M.-C.; Neufeld, E.; Moser, H.; Huber, E.; Farcito, S.; Gerber, L.; Jedensjö, M.; Hilber, I.; Di Gennaro, F.; Lloyd, B.; et al. Development of a new generation of high-resolution anatomical models for medical device evaluation: The Virtual Population 3.0. *Phys. Med. Biol.* **2014**, *59*, 5287–5303. [[CrossRef](#)] [[PubMed](#)]
43. Feliziani, M. Subcell FDTD Modeling of Field Penetration Through Lossy Shields. *IEEE Trans. Electromagn. Compat.* **2011**, *54*, 299–307. [[CrossRef](#)]
44. Feliziani, M.; Maradei, F. Circuit-oriented FEM: Solution of circuit-field coupled problems by circuit equations. *IEEE Trans. Magn.* **2002**, *38*, 965–968. [[CrossRef](#)]
45. Buccella, C.; Feliziani, M.; Maradei, F.; Manzi, G. Magnetic field computation in a physically large domain with thin metallic shields. *IEEE Trans. Magn.* **2005**, *41*, 1708–1711. [[CrossRef](#)]
46. Feliziani, M.; Maradei, F. Fast computation of quasi-static magnetic fields around nonperfectly conductive shields. *IEEE Trans. Magn.* **1998**, *34*, 2795–2798. [[CrossRef](#)]
47. Feliziani, M.; Maradei, F. Edge element analysis of complex configurations in presence of shields. *IEEE Trans. Magn.* **1997**, *33*, 1548–1551. [[CrossRef](#)]

**Disclaimer/Publisher’s Note:** The statements, opinions and data contained in all publications are solely those of the individual author(s) and contributor(s) and not of MDPI and/or the editor(s). MDPI and/or the editor(s) disclaim responsibility for any injury to people or property resulting from any ideas, methods, instructions or products referred to in the content.